Jurnal Teknologi

Full Paper

NIGHT TIME CLOUDS DETECTION ABOVE PERMATAPINTAR OBSERVATORY USING ALL-SKY IMAGERY

Mohammad Afiq Dzuan Mohd Azhar[a,b], Nurul Shazana Abdul Hamid[b*], Wan Mohd Aimran Wan Mohd Kamil[a], Nor Sakinah Mohamad[b]

[a]Department of Applied Physics, Faculty of Science and Technology, Universiti kebangsaan Malaysia, 43600 UKM Bangi, Selangor, Malaysia
[b]Pusat GENIUS@Pintar Negara, Universiti Kebangsaan Malaysia, 43600 UKM Bangi, Selangor, Malaysia

Article history
Received
16 November 2021
Received in revised form
15 June 2022
Accepted
25 July 2022
Published Online
31 October 2022

*Corresponding author
zana@ukm.edu.my

Graphical abstract

Abstract

We proposed a method to detect clouds in a suburban class night sky for the larger purpose of astronomical site testing. A 'threshold criterion' approach was adopted to discriminate between the pixels representing the foreground clouds from the pixels representing the background sky in a single all-sky image. This method was developed based on all-sky images captured at the PERMATApintar Observatory (PpO) in Selangor (2°55'02" N, 101°47'17" E), where the night sky has been categorised as a suburban class night sky. The night sky conditions were divided into three categories depending on the cloud cover: clear, partially cloudy, and overcast skies. Samples of all-sky images for each night sky condition were selected and respective histogram images were generated. These samples were then used to inductively derive the threshold criterion based on the skewness and peak values of the image's histogram. This sky/cloud threshold will enable pixels representing foreground clouds to be discriminated from the pixels representing the background sky under each type of night sky conditions. Our work found that the night sky over PpO requires two thresholds to accurately distinguish between cloud and sky pixels due to the sky glow effect. The first threshold is based on the peak value of the image's histogram. If an image's histogram has a peak value ≥ 80, then the image is considered a clear sky. Otherwise, the image is considered cloudy or overcast sky if the peak value is < 80. The second threshold value is dependent on the night sky condition determined by the first threshold. The sky/cloud threshold value for a clear and cloudy sky is 80 and 180, respectively. If a pixel has a pixel value equal to or greater than the respective thresholds, the pixel will be considered a sky pixel and vice versa.

Keywords: Nighttime Cloud detection, all-sky images, threshold, histogram, pixel analysis

Abstrak

Kami mengusulkan sebuah kaedah mengesan awan pada waktu malam untuk langit yang tergolong dalam kelas pinggir bandar bagi tujuan ujian tapak cerapan astronomi. Pendekatan 'kriteria nilai ambang' telah digunakan untuk membezakan piksel awan daripada piksel langit malam dalam imej seluruh-langit. Kaedah ini dibangunkan berdasarkan imej

seluruh-langit yang ditangkap di PERMATApintar Observatory (PpO), Selangor (2°55'02" N, 101°47'17" E), di mana langitnya tergolong dalam kelas langit malam pinggir bandar. Keadaan langit malam di bahagikan kepada tiga kategori bergantung kepada jumlah liputan awan: tidak berawan, separa berawan, dan berawan penuh. Sampel-sampel bagi imej seluruh-langit untuk setiap keadaan langit telah dipilih dan histogram imej telah dijana. Histogram imej ini kemudiannya digunakan untuk menentukan kriteria nilai ambang berdasarkan kepencongan dan nilai puncaknya. Nilai ambang langit-awan ini akan membolehkan piksel awan dibezakan daripada piksel langit bagi setiap keadaan langit. Kajian kami mendapati bahawa langit malam di PpO memerlukan dua nilai ambang bagi membezakan piksel awan daripada piksel langit latar dengan lebih tepat akibat kesan teja langit. Kedua-dua nilai ambang ini diaplikasikan secara berturutan. Nilai ambang pertama ditentukan berdasarkan nilai puncak bagi histogram imej. Sekiranya histogram imej mempunyai nilai puncak ≥ 80, maka imej tersebut akan dianggap sebagai langit malam yang tidak berawan. Sebaliknya, imej akan dianggap sebagai separa berawan atau berawan penuh sekiranya nilai puncak < 80. Nilai ambang kedua pula adalah bergantung kepada keadaan langit malam yang telah ditentukan oleh nilai ambang pertama. Bagi keadaan langit yang tidak berawan, nilai ambang kedua ialah 80, manakala bagi keadaan langit yang separa berawan atau berawan penuh, nilai ambang ialah 180. Jika sebuah piksel mempunyai nilai piksel yang sama atau lebih besar daripada nilai ambang untuk kedua-dua kes langit tidak berawan ataupun langit separa berawan/langit berawan penuh, maka piksel tersebut akan dikelaskan sebagai piksel langit.

Kata kunci: Kaedah mengesan awan pada waktu malam imej seluruh langit, nilai ambang, histogram,piksel langit,

1.0 INTRODUCTION

Cloud coverage is one of the most vital parameters in astronomical site testing and monitoring [1,2,3,4]. Long-term cloud coverage data is crucial for astronomical observation time and maintenance, especially for astronomical sites within the equatorial region, where there are extensive cloud cover. Generally, cloud coverage can be measured using ground-based techniques or satellite-based measurement [5]. A long-term cloud coverage is best obtained from satellite images. However, satellite data requires suitable and high spatial resolution [6,7]. In addition, specific astronomical sites might require very high spatial resolution satellite data, especially during nighttime due to its unique geographical conditions [5]. Due to this, ground-based measurements are still vital for final site assessment [2].

Ground-based measurements can be conducted in several ways. The basic yet less accurate method is through naked-eye observation. The lack of accuracy is due to the human factor – more experienced observers will most likely produce better data. In order to remove the human factor, an all-sky camera is used to measure cloud coverage quantitatively, which provides better accuracy and consistency. All-sky camera systems such as the Hemispherical Sky Imager/ Total Sky Imager and Whole Sky Imager have been developed for such purposes using a high-resolution sensor [8, 9, 10, 11]. There are also all-sky camera systems that utilize simple commercial instruments such as DSLR cameras with a fisheye lens [12, 13], low resolution commercial all-sky cameras [14, 15], compact digital camera [16, 17] and some even using a smartphone camera [18].

Generally, cloud detection can be categorized into two types: daytime and nighttime measurement, depending on the research purpose. Daytime cloud detection has been widely studied and explored. It has been done using many different instruments and setups based on specific studies or localized needs. The algorithm development for daytime cloud detection have also been upgraded from time to time to optimize cloud detection, resulting in better accuracy in cloud coverage measurements. Daytime cloud measurement is important to many fields such as meteorology [19, 20, 21], climatology [22], solar radiation study [23, 24, 25], ecological and environmental studies [26, 13], and astronomy [28, 29, 30].

Nighttime cloud measurement is not as well-known as daytime measurements. This is because its application is limited to a few fields, such as ecological and astronomical study [15]. In astronomy, cloud coverage study falls under astroclimatology. This is a branch of astronomy that focuses on sky quality evaluation based on techniques and instrumentations. Astroclimatology investigates the relationship between meteorological parameters and the observational condition through the application

of the theories of electromagnetic waves propagation in turbulent media [32]. It is further categorized into four main parameters: observational, meteorological, geographical, and seismological parameters [33].

The night sky has very different characteristics compared to the daytime sky. Thus, most of the daytime cloud coverage measurement methods cannot be properly utilized at night. Therefore, new approaches have been developed to detect and measure clouds during nighttime. Several astronomical observatories used infrared instruments to measure cloud coverage [34, 35]. However, this method can only be used by high profile observatories due to its expensive cost. Some observatories utilized stars to detect the presence of clouds on the night sky [36]. However, this method required a very dark sky. A brighter night sky will outshine the stars causing them to be less visible at the night sky. This condition will lead to inaccurate cloud detection compared to a dark night sky because there is another factor that conceals the stars. It has caused observatories located in the area with high light pollution to face difficulties in measuring and assessing nighttime cloud coverage.

This paper proposes a new method of nighttime cloud detection specifically for astronomical observatories with high night sky brightness.

2.0 THE SITE: PERMATApintar OBSERVATORY (PpO)

The PERMATApintar Observatory (PpO) is located within Universiti Kebangsaan Malaysia, Selangor, Malaysia (2°55'02" N, 101°47'17" E). Initially, the main purpose of the observatory is for astronomical education for gifted and talented students. However, the observatory is currently venturing into astronomical research opportunities. In order to accomplish that, a series of astroclimatological studies are being conducted to determine what kind of astronomical studies can be conducted at the observatory.

Due to its location in a suburban area, the night sky over the observatory is bright. Studies by Azmi *et al.*, (2020) and Azhar *et al.*, (2016) showed that the darkest night sky is around 18-19 mag/sec2 [37,38]. This night sky condition makes cloud coverage measurement based on star detection unsuitable at PpO. In addition, cloud coverage measurement using non-visual instruments such as radio or infrared devices will require a very large cost.

These astroclimatogical studies for PpO is very crucial to characterize its sky due to no astronomical site testing has been done before it was constructed. By knowing such information, we can utilize it to determine what kind of astronomical research can we focus on and when the best time to do it. Long term cloud coverage is among the main parameter to determine the above questions.

3.0 THEORY

The appearance of the night sky can vary at different locations. Sites in rural regions are most likely to have a dark night sky, whereas sites located in nearby cities will have a brighter night sky. In general, when we compare both images taken from both sites, we can see that the overall difference is the intensity of pixel value. The darker night will have lower intensity of pixel number for all red, green and blue colour channels and vice versa. It is also important to mention that the intensity for red, green and blue are also more or less the same, unlike the bluish sky during the daytime (where blue dominates compared to green and red). Since the daytime cloud detection algorithm is based on the difference or ratio between the colour channels, nighttime cloud detection cannot simply emulate daytime methods.

The location of PpO near several major cities has caused the night sky to brighten and outshine many dimmer stars. The excess lights brighten up the night sky and greatly intensify the cloud brightness due to light scattering. Theoretically, there will be no significant difference in terms of intensity between each colour channel. However, we have found that there are apparent differences in intensity between the night sky and the cloud. Figure 1 shows the bright up cloud due to light pollution over PpO. By utilizing the difference between the intensity of the cloud and the night sky, an algorithm can be developed to detect clouds and then measure the cloud coverage.

4.0 METHODOLOGY

This section includes discussion on all-sky camera and images, images preprocessing, threshold determination and the algorithm. Also include discussion on regarding the Moon-pixel problem. The methodology can summarize as shown in Figure 2 below.

(a) (b) (c)

Figure 1 All-sky images for (a) clear, (b) partially cloudy and (c) overcast night sky conditions

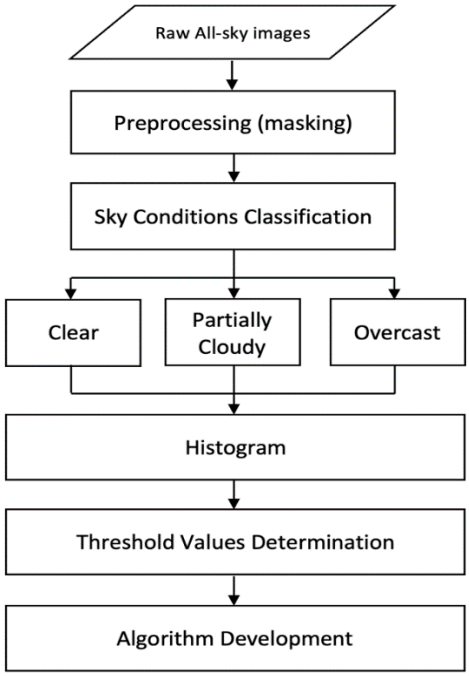

Figure 2 Methodology flowchart

4.1 All-Sky Camera and Images

The nighttime all-sky images are obtained from the all-sky image database at the PERMATApintar Observatory. The images are taken using an all-sky camera located next to the observatory. The all-sky camera is initially used for real-time sky monitoring from the observatory. It records hemispherical all-sky images on an hourly basis. Table 1 shows the specifications of the all-sky camera. Sixty all-sky images from the observatory's database have been chosen between May 2013 and May 2016. The images mainly consist of clear, partially cloudy and overcast sky conditions.

Table 1 Camera Specifications [39]

All-Sky Camera (ASC-N1)	
Image Sensor	1/3" Sony Super HAD CCD II
Picture Size	546 x 457 pixels
Field of View	190°
Projection	Circular fisheye
Exposure time	1/1000000 – 4 seconds
Limiting stellar magnitude	Approx. magnitude 4
Len's focal length	1.24 mm
Len's f-stop	f/2.8
weight	0.3 kg

4.2 Images Preprocessing

The chosen all-sky images will be preprocessed before any further analysis are done. The preprocessing part is mainly included image masking. A mastermask is generate based on the all-sky images. Basically, a mastermask is a binary image, where pixels with pixel value of zero are pixels that represent a non-sky: building, trees, poles etc that blocking the sky. On the other hand, the pixel value of one will represent the sky. Since mastermask and all-sky image are basically a matrice of pixel values, a product between both of them will produce a clean all-sky image.

4.3 Threshold Value

In this study, we utilize a histogram of the clean all-sky image to evaluate the characteristic of pixel numbers for each sky conditions. The skewness and peak of the histograms are compared to observe and identify the trends for each sky condition. A threshold can be determined based on the peak values of the histograms. This threshold value is essential for developing an algorithm to identify and measure cloud coverage from the all-sky images.

4.4 Algorithm

The algorithm consists of three main parts: pre-processing, pixel identification, and cloud coverage measurement. The pre-processing part is essential for removing unwanted information other than the all-sky image's region of interest (ROI). This process also included masking any pixels representing neither the sky nor the cloud, such as trees, buildings and lighting poles. A Mastermask that covers the non-ROI pixels and those that do not represent sky and cloud is created and applied onto the raw image to produce a clean all-sky image. The Mastermask is a binary image with an identical size to the raw all-sky images. The covered region is represented by pixels with a pixel value of 0, while the rest is a pixel value of 1. Both Mastermask and raw all-sky images can be considered as two huge, identically-sized matrices. A detailed explanation of these masking processes can be found in the previous study by Azhar *et al.*, (2021) [15].

The pixel identification part is mainly about distinguishing between sky-pixel and cloud-pixel within the ROI region. The sky and cloud pixels are determined using the threshold value specifically for the night sky over the observatory. The third part, the cloud coverage measurement, is conducted by calculating the total numbers of sky-pixel and cloud-pixel. The cloud cover will be measured in terms of percentage using the following equations:

$$Cloud\ coverage\ percentage, CCP = \frac{N_{cloud}}{N_{ROI}} \times 100\%$$

where N_cloud is the number of sky pixels while N_ROI is the number of pixels in the ROI. The N_ROI for each all-sky image can also be determined from the summation of the total number of cloud-pixel and sky-pixel.

4.5 The Moon-pixels

One problem face by our method is the present of the Moon during clear night sky. The All-sky camera in PpO is not properly design to exclude the moon since it mainly for live-monitoring purposes.

The pixels that represent the Moon will have high pixel values. Thus, the algorithm will recognize them as cloud-pixel. Since the cloud coverage percentage is based on okta scale, the all-sky image of a clear night clear with the present of The Moon will still consider as a clear night sky due to the moon covered less than 10% of the total pixels in the region of interest of the images.

5.0 RESULT AND DISCUSSION

This section will discuss the threshold values determination and final algorithm development. It also includes the obstacles faced during threshold values determination, such as the sky glow and the solution to overcome it.

5.1 Determination of Threshold Value and Algorithm Development

The histograms of all-sky images show an apparent trend regarding the peak histogram value of each night sky condition. Figure 3 shows the examples of the histograms for all three sky conditions. Most of the images have a histogram that is skewed to the right. However, the histograms for the clear sky images show a peak value located far to the left. In contrast, both partially cloudy and overcast night sky conditions have peak values that are situated close to the center of the histogram. The peak of the histogram for overcast sky conditions is located slightly to the right side

These trends can be related to the characteristic of the night sky over PpO. Most of the pixels in clear night sky images are sky pixels, and they mostly have a low intensity of pixel value. Therefore, the histogram is skewed to the right. In overcast night sky conditions, the pixels are all cloud pixels. Since clouds in a light-polluted area are bright, the cloud pixels will have a higher pixel value, thus causing the histogram to skew to the right. Based on this trend, the threshold value can determine from the peak values of the histogram.

Even though most pixels of each colour channel have approximately the same pixel value, there are some cases where the pixel values are different. Therefore, we used the average histogram peak value for each color channel and compared all the average histogram peak values to determine the threshold value. Figure 4 shows the comparison of the average histogram peak values for each of the all-sky

images. The average histogram peak values for partially cloudy and overcast sky conditions do not display a discernible trend. However, the average histogram peak values for clear sky conditions have a consistent characteristic: the average values are always lower than the values of the two other sky conditions. For our study, we decided to find the mid-value between the lower average histogram peak value of either partial cloudy or overcast sky condition and the highest average histogram peak value for the clear sky condition. The mid-value is then utilized as the threshold value. In this study, we have found that the threshold value is 80, where pixels with pixel values higher than 80 will be considered a cloud-pixel and those with pixel values equal to or lower than 80 will be considered sky-pixel. This threshold value will be called as sky/cloud threshold for the rest of the paper.

We also have encountered one more factor that affects pixel identification which is sky glow. This phenomenon can be seen clearly in the all-sky images as a glowing region near the horizon. It can also be detected in the histogram as the second peak. The algorithm which used a threshold value of 80 will consider sky-pixels in the sky glow region as clouds and cause a major error in cloud coverage measurement. To overcome the problem, the algorithm needs to utilize two stages threshold method. The first stage is to fix the sky glow problem, and the second stage is to distinguish each pixel using a specific threshold value determined in the first stage.

Based on the images and histograms, the presence of sky glow is very dominant in clear sky conditions compared to other sky conditions. Therefore, the primary purpose of the first stage is to determine whether the all-sky image is a clear sky condition or not. The determination can be done by utilizing the histogram of the images. The histogram alone can indirectly tell us which type of pixels is dominating the images. For instance, if the histogram peak is located to the left-hand side, it means that most of the image pixels are sky-pixel. Thus, it can be considered that the image is an image of a clear night sky. Based on that, the first stage will utilize the sky/cloud threshold to determine the condition of the night sky. If an image's average histogram peak value is equal to or lower than 80, the image will be considered as a clear night sky and vice versa.

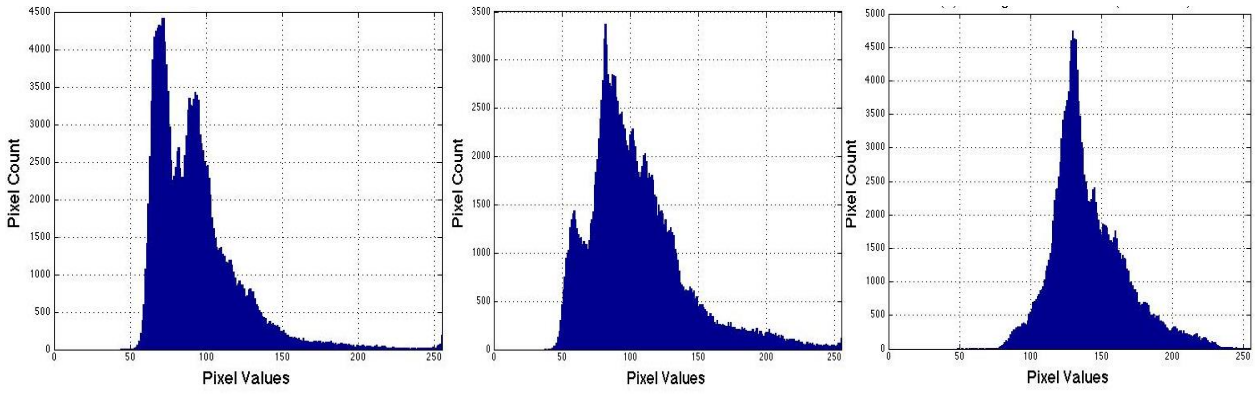

(a) (b) (c)

Figure 3 The histograms for the all-sky images of (a) clear sky, (b) partially cloudy and (c) overcast night sky

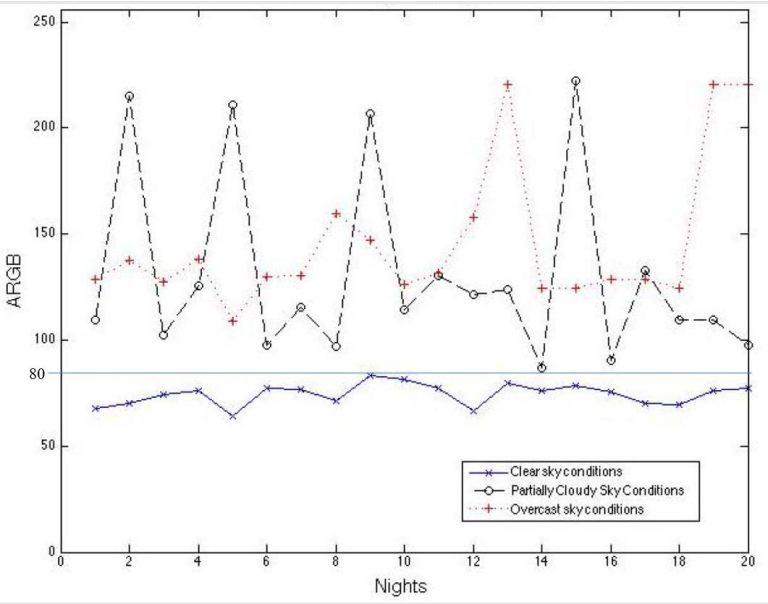

Figure 4 The average histogram peak value comparison for each night sky conditions. Straight solid horizontal blue line indicates the threshold value to distinguish between clear and cloudy sky condition

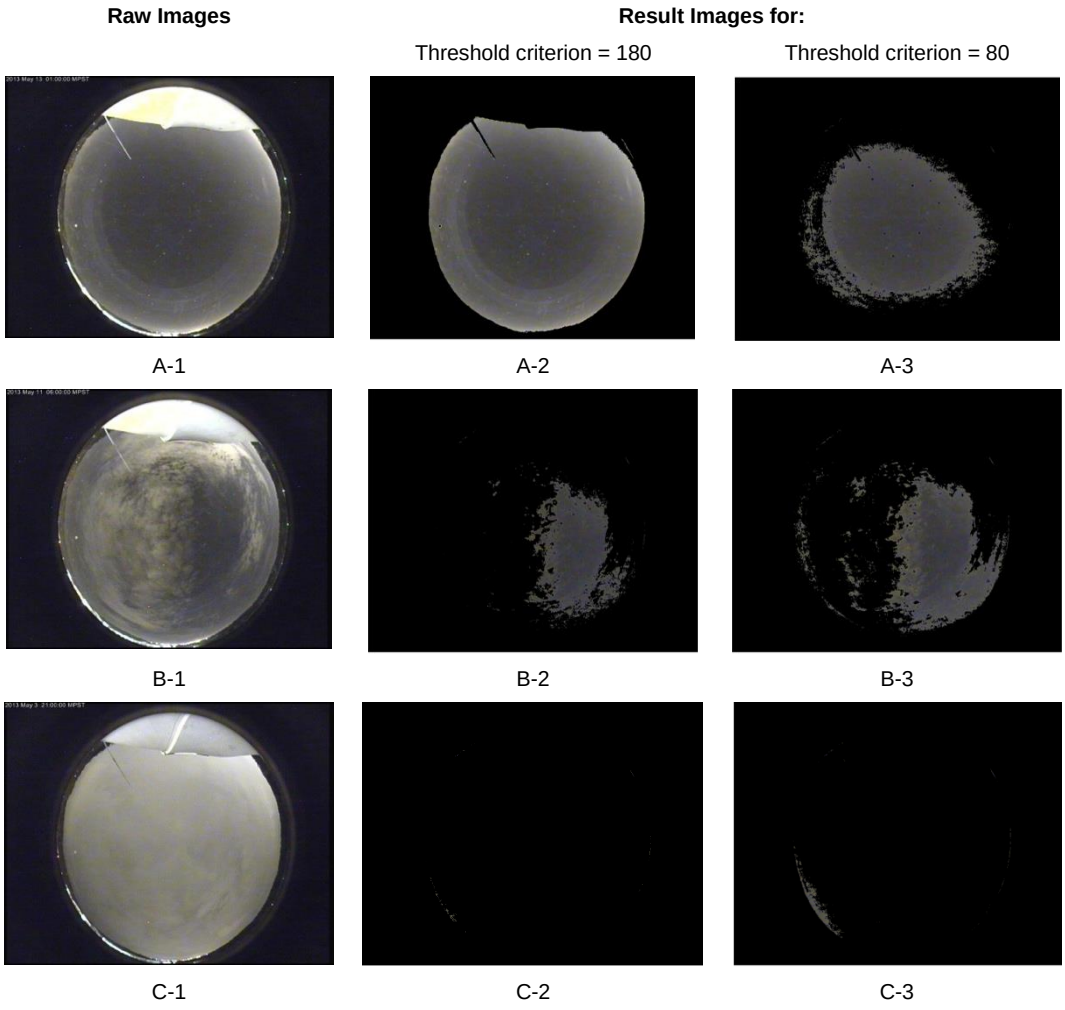

Figure 5 The raw all-sky image (left) and the post processing image for sky/cloud threshold value of 180 (middle) and 80 (right) for clear (A1-3), partially cloudy (B1-3) and overcast (C1-3) night sky condition

The second stage will use different sky/cloud threshold values based on the night sky condition determined in the first stage. As for all-sky images that have been considered as the non-clear sky (partial cloudy or overcast sky condition), the pixels distinguishing process will be using the original sky/cloud threshold value of 80. However, clear sky images must use different sky/cloud threshold values to account for the sky glow. Based on the histograms, the variation of the second histogram peaks is observed and used as the lower limit for the threshold value. Through our trial-and-error process, a suitable and workable value have been determined. The sky/cloud threshold for the clear sky images in the second stage is 180, where pixel with pixel value equal to or lower to 180 will consider as a sky-pixel and vice versa. Figure 5 shows how sky glow affects cloud detection and the effectiveness of both sky/cloud threshold values in detection pixels in different sky conditions. The sky/cloud threshold of 180 can overcome the sky glow effect almost perfectly. However, the threshold will cause over-detection of cloud-pixel for both partially cloudy and overcast sky conditions. Meanwhile, the sky/cloud threshold of 80 will show over-detection of cloud-pixel due to sky glow for sky clear images but no issues in cloud-pixel detection for the other two sky conditions.

Since our detection method required two threshold values, thus a two-stage algorithm must be developed. The algorithm worked by scanning each of the pixels in the images, column by column. Each pixel will go through all-sky image masking process (pre-process), sky condition determination (stage one) and pixel distinguishing processes (stage two) before the cloud coverage measurement is completed. Figure 6 shows the flow chart of the algorithm.

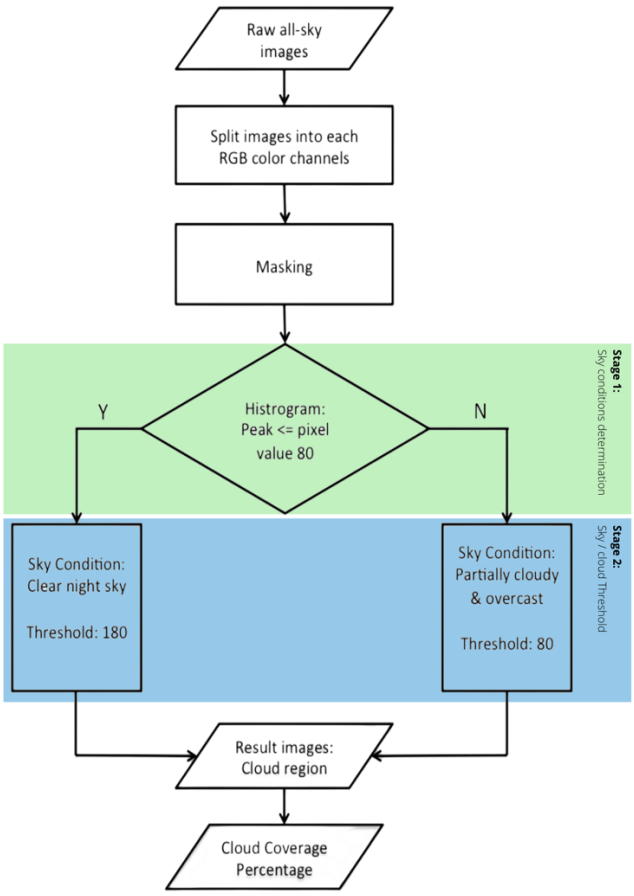

Figure 6 The flowchart for the nighttime cloud detection and coverage measurement. The green region shows the first stage threshold (sky condition determination) and the blue region shows the second threshold (sky/cloud threshold)

6.0 CONCLUSION

This study has developed a two-stage method for nighttime cloud detection and coverage measurement for the night sky over PERMATApintar Observatory. The two-stage method is proposed to overcome a local sky glow from causing over-detection of cloud-pixel, especially for clear night sky images. Our study has shown that the sky glow effects are very dominant in clear sky images only. Therefore, the first stage is mainly to determine the night sky condition of the all-sky images. The second stage utilises the night sky condition determination in the first stage to determine which sky/cloud threshold values to be used for pixel discrimination. The sky/cloud threshold of 80 will be used for partially cloudy and overcast sky conditions, while the threshold of 180 will be used for clear sky conditions. By introducing specialised threshold values for cloud-sky discrimination that are sensitively tailored to the night sky conditions instead of forcing a general threshold method, we are on a promising path to develop a nighttime cloud detection method with sufficient operational flexibility to work under any sky conditions.

Acknowledgement

The authors would like to express our gratitude to GENIUS@Pintar National Gifted Centre for the permission to access PERMATApintar Observatory's All-Sky Images Database.

References

[1] Schöck, M., Els, S., Riddle, R., Skidmore, W., Travouillon, T., Blum, R., and Wang, L. 2009. Thirty Meter Telescope Site Testing I: Overview. *Publications of the Astronomical Society of the Pacific*. 121(878): 384. DOI: https://doi.org/10.1086/599287.

[2] Cao, Z. H. *et al*. 2020. Long-Term Analysis of Clear Nights Using Satellite Data Considering Astronomical Sites in Western China. *Research in Astronomy and Astrophysics*. 20(6): 081 DOI: https://doi.org/10.1088/1674-4527/20/6/81.

[3] Aksaker, N. A. Z. I. M., Yerli, S. K., Erdoğan, M. A., Kurt, Z., Kaba, K., Bayazit, M., and Yesilyaprak, C. 2020. Global Site Selection for Astronomy. *Monthly Notices of the Royal Astronomical Society*. 493(1): 1204-1216. DOI: https://doi.org/10.1093/mnras/staa201.

[4] Kazım, K. A. B. A., YEŞİLYAPRAK, C., and ŞATIR, O. 2021. A New Astronomical Parameter from Remote Sensing Data:

Astronomical Clearness Index (ACI). *Communications Faculty of Sciences University of Ankara Series A2-A3 Physical Sciences and Engineering*. 63(1): 58-79.
DOI: https://doi.org/10.33769/aupse.85149.

[5] Vernin, J., Muñoz-Tuñón, C., Sarazin, M., Ramió, H. V., Varela, A. M., Trinquet, H., and Vrech, R. 2011. European Extremely Large Telescope Site Characterization I: Overview. *Publications of the Astronomical Society of the Pacific*. 123(909): 1334.
DOI: https://doi.org/10.1086/662995.

[6] Kurlandczyk, H., and Sarazin, M. 2007. Remote Sensing of Precipitable Water Vapour and Cloud Cover for Site Selection of the European Extremely Large Telescope (E-ELT) Using MERIS. In Remote Sensing of Clouds and the Atmosphere XII). *International Society for Optics and Photonics.* 6745: 674507.
DOI: https://doi.org/10.1117/12.736820.

[7] Varela, A. M., Bertolin, C., Muñoz-Tuñón, C., Ortolani, S., and Fuensalida, J. J. 2008. Astronomical Site Selection: On the Use of Satellite Data for Aerosol Content Monitoring. *Monthly Notices of the Royal Astronomical Society*. 391(2): 507-520.
DOI: https://doi.org/10.1111/j.1365-2966.2008.13803.x.

[8] Pfister, G., McKenzie, R. L., Liley, J. B., Thomas, A., Forgan, B. W., and Long, C. N. 2003. Cloud Coverage Based on All-Sky Imaging and Its Impact on Surface Solar Irradiance. *Journal of Applied Meteorology and Climatology* 42(10): 1421-1434.
DOI: https://doi.org/10.1175/1520-0450.

[9] Long, C. N., Sabburg, J. M., Calbó, J., and Pagès, D. 2006. Retrieving Cloud Characteristics from Ground-Based Daytime Color All-Sky Images. *Journal of Atmospheric and Oceanic Technology*. 23(5): 633-652.
DOI: https://doi.org/10.1175/JTECH1875.1.

[10] Calbo, J., and Sabburg, J. 2008. Feature Extraction from Whole-Sky Ground-Based Images for Cloud-Type Recognition. *Journal of Atmospheric and Oceanic Technology*. 25(1): 3-14.
DOI: https://doi.org/10.1175/2007JTECHA959.1.

[11] Heinle, A., Macke, A., and Srivastav, A. 2010. Automatic Cloud Classification of Whole Sky Images. *Atmospheric Measurement Techniques* 3(3): 557-567.
DOI: https://doi.org/10.5194/amt-3-557-2010.

[12] Jechow, A., Kolláth, Z., Ribas, S. J., Spoelstra, H., Hölker, F., and Kyba, C. 2017. Imaging and Mapping the Impact of Clouds on Skyglow with All-Sky Photometry. *Scientific Reports* 7(1): 1-10.
DOI: https://doi.org/10.1038/s41598-017-06998-z.

[13] Jechow, A., Hölker, F., and Kyba, C. C. 2019. Using All-Sky Differential Photometry to Investigate How Nocturnal Clouds Darken the Night Sky in Rural Areas. *Scientific Reports.* 9(1): 1-14.
DOI: https://doi.org/10.1038/s41598-018-37817-8.

[14] Sun, S., Ernst, J., Sapkota, A., Ritzhaupt-Kleissl, E., Wiles, J., Bamberger, J., and Chen, T. 2014. Short Term Cloud Coverage Prediction Using Ground Based All Sky Imager. *2014 IEEE International Conference on Smart Grid Communications (SmartGridComm)*.121-126.
DOI: https://doi.org/10.1109/SmartGridComm.2014.7007633.

[15] Azhar, M. A. D. M., Hamid, N. S. A., Kamil, W. M. A. W. M., and Mohamad, N. S. 2021. Daytime Cloud Detection Method Using the All-Sky Imager Over Permatapintar Observatory. *Universe*. 7(2): 41.
DOI: https://doi.org/10.3390/universe7020041.

[16] Tzoumanikas, P., Nikitidou, E., Bais, A. F., and Kazantzidis, A. 2016. The Effect of Clouds on Surface Solar Irradiance, Based on Data from an All-Sky Imaging System. *Renewable Energy*. 95: 314-322.
DOI: https://doi.org/10.1016/j.renene.2016.04.026.

[17] Kazantzidis, A., Tzoumanikas, P., Bais, A. F., Fotopoulos, S., and Economou, G. 2012. Cloud Detection and Classification with the Use of Whole-Sky Ground-Based Images. *Atmospheric Research*. 113: 80-88.
DOI: https://doi.org/10.1016/j.atmosres.2012.05.005.

[18] Parisi, A. V., Downs, N., Igoe, D., and Turner, J. 2016. Characterization of Cloud Cover with a Smartphone Camera. *Instrumentation Science & Technology*. 44(1): 23-34.
DOI: https://doi.org/10.1080/10739149.2015.1055577.

[19] Huo, J., and Lu, D. 2009. Cloud Determination of All-Sky Images Under Low-Visibility Conditions. *Journal of Atmospheric and Oceanic Technology*. 26(10): 2172-2181.
DOI: https://doi.org/10.1175/2009JTECHA1324.1.

[20] Wacker, S., Groebner, J., Zysset, C., Diener, L., Tzoumanikas, P., Kazantzidis, A., and Kaempfer, N. 2015. Cloud Observations in Switzerland Using Hemispherical Sky Cameras. *Journal of Geophysical Research: Atmospheres*. 120(2): 695-707.
DOI: https://doi.org/10.1002/2014JD022643.

[21] Aebi, C., Gröbner, J., Kämpfer, N., and Vuilleumier, L. 2017. Cloud Radiative Effect, Cloud Fraction and Cloud Type at Two Stations in Switzerland Using Hemispherical Sky Cameras. *Atmospheric Measurement Techniques.* 10(12): 4587-4600.
DOI: https://doi.org/10.5194/amt-10-4587-2017.

[22] Bendix, J., Rollenbeck, R., and Palacios, W. E. 2004. Cloud Detection in the Tropics--A Suitable Tool for Climate-Ecological Studies in the High Mountains of Ecuador. *International Journal of Remote Sensing*. 25(21): 4521-4540.
DOI: https://doi.org/10.1080/01431160410001709967.

[23] Zain-Ahmed, A., Sopian, K., Abidin, Z. Z., and Othman, M. Y. H. 2002. The Availability of Daylight from Tropical Skies—A Case Study of Malaysia. *Renewable Energy*. 25(1): 21-30.
DOI: https://doi.org/10.1016/S0960-1481(00)00209-3.

[24] Alonso-Montesinos, J., Batlles, F. J., and Portillo, C. 2015. Solar Irradiance Forecasting at One-Minute Intervals for Different Sky Conditions Using Sky Camera Images. *Energy Conversion and Management.* 105: 1166-1177.
DOI: https://doi.org/10.1016/j.enconman.2015.09.001.

[25] Cazorla, A., Husillos, C., Antón, M., and Alados-Arboledas, L. 2015. Multi-Exposure Adaptive Threshold Technique for Cloud Detection with Sky Imagers. *Solar Energy*. 114: 268-277.
DOI: https://doi.org/10.1016/j.solener.2015.02.006.

[27] Trlica, A., Hutyra, L. R., Schaaf, C. L., Erb, A., and Wang, J. A. 2017. Albedo, Land Cover, and Daytime Surface Temperature Variation Across an Urbanized Landscape. *Earth's Future*. 5(11): 1084-1101.
DOI: https://doi.org/10.1002/2017EF000569.

[28] Yang, Y., Moore, A. M., Krisciunas, K., Wang, L., Ashley, M. C., Fu, J., and Zhu, Z. 2017. Optical Sky Brightness and Transparency During the Winter Season at Dome a Antarctica from the Gattini-All-Sky Camera. *The Astronomical Journal.* 154(1): 6.
DOI: https://doi.org/10.3847/1538-3881/aa73dc.

[29] Klinglesmith III, D. A., Buscher, D., Creech-Eakman, M. J., Etscorn, D., Garcia, E., and Gino, C. 2018. Weather Trends at The Magdalena Ridge Observatory. In Observatory Operations: Strategies, Processes, and Systems VII. *International Society for Optics and Photonics*. 10704: 107042B
DOI: https://doi.org/10.1117/12.2312682.

[30] Chytka, L., Mandat, D., Albury, J., Bellido, J. A., Farmerh, J., Fujii, T., and Vacula, M. 2020. An Automated All-Sky Atmospheric Monitoring Camera for a Next-Generation Ultrahigh-Energy Cosmic-Ray Observatory. *Journal of Instrumentation.* 15(10): T10009.
DOI: https://doi.org/10.1088/1748-0221/15/10/T10009.

[31] Azhar, M. A. D. M., Hamid, N. S. A., Kamil, W. M. A. W. M., & Mohamad, N. S. 2019. Urban Night Sky Conditions Determination Method Based on a Low-Resolution All-Sky Images. *2019 6th International Conference on Space Science and Communication (IconSpace)*. 158-162.
DOI: https://doi.org/10.1109/IconSpace.2019.8905975.

[32] Lombardi, G. 2009. Astronomical Site Testing in the Era of the Extremely Large Telescopes.
DOI: https://doi.org/10.6092/unibo/amsdottorato/2031.

[33] European Southern Observatory. Paranal Astroclimatology. 2018.https://www.eso.org/sci/facilities/paranal/astroclimate.html.

[34] Redman, B. J., Shaw, J. A., Nugent, P. W., Clark, R. T., and Piazzolla, S. 2018. Reflective All-Sky Thermal Infrared Cloud Imager. *Optics Express*. 26(9): 11276-11283. DOI: https://doi.org/10.1364/OE.26.011276.
[35] Wang, Y., Liu, D., Xie, W., Yang, M., Gao, Z., Ling, X., and Xia, Y. 2021. Day and Night Clouds Detection Using a Thermal-Infrared All-Sky-View Camera. *Remote Sensing*. 13(9): 1852. DOI: https://doi.org/10.3390/rs13091852.
[36] Mandeville, W. J., McLaughlin, T., Bygren, S., and Randell, C. 2015. Visible Cloud Imager for Autonomous Telescopes. *Proceedings of the AMOS*. Technical Conference.
[37] Azmi, N. C., Kamil, W. M. A. W. M., & Azhar, M. A. D. M. 2021. An All-Sky Map of Night Sky Brightness at Pusat Permatapintar® Negara. *AIP Conference Proceedings*. 2319(1): 040016. DOI: https://doi.org/10.1063/5.0036983.
[38] Azhar, A. D., Gopir, G., Kamil, W. W. M., Mohamad, N. S., & Azmi, N. C. 2016. Night Sky Brightness Measurement at Permatapintar Observatory. *AIP Conference Proceedings*. 1784(1): 040003. DOI: https://doi.org/10.1063/1.4966789.
[39] Moonglow Technologies. 2020. All Sky Cam. http://www.moonglowtech.com/products/AllSkyCam/Specifications.shtml.